



Near-infrared chemical imaging (NIR-CI) for counterfeit drug identification—A four-stage concept with a novel approach of data processing (Linear Image Signature)

T. Puchert^a, D. Lochmann^b, J.C. Menezes^c, G. Reich^{a,*}

^a Institute of Pharmacy and Molecular Biotechnology, Department of Pharmaceutical Technology and Biopharmaceutics, University of Heidelberg, Im Neuenheimer Feld 366, D-69120 Heidelberg, Germany

^b Quality Operations, PAT – Laboratory, Merck Serono, Darmstadt, Germany

^c Institute of Biotechnology and Bioengineering, IST, Technical University of Lisbon, Portugal

ARTICLE INFO

Article history:

Received 11 June 2009

Received in revised form 4 August 2009

Accepted 18 August 2009

Available online 26 August 2009

Keywords:

NIR-CI

NIRS

Counterfeits

QbD

MVA

Homogeneity

ABSTRACT

A new stage concept was developed to reliably identify counterfeit tablets which are very similar to the genuine drug product. This concept combines single-point near-infrared spectroscopy (NIRS) and near-infrared chemical imaging (NIR-CI) with statistical variance analysis. The advantage of NIR-CI over NIRS is the potential to determine not only the amount, but also the spatial distribution of ingredients within a single tablet. Previously published NIR-CI studies used homogeneity as a key indicator for the identification of counterfeits. The state of the art approach for estimating homogeneity is to record the average and % standard deviation of predicted classification scores (i.e. concentrations) for a given component within a specimen. A disadvantage of this approach is the partial loss of spatial information. In view of this, we developed a new method using much more of the spatial information for the estimation of homogeneity. The method is based on (1) summation and unfolding of multidimensional predicted classification scores, which results in a Linear Image Signature (LIS) and (2) multivariate LIS data analysis (LIS-MVA). It could be demonstrated that this kind of NIR-CI data analysis represents an innovative approach for the identification of counterfeit tablets. Moreover, this procedure is applicable to determine the product variability, i.e. process signature of a given product thus being a valuable tool within the Quality by Design (QbD) approach of the ICH Q8 guideline.

© 2009 Elsevier B.V. All rights reserved.

1. Introduction

In recent years, the number of counterfeit drug products has increased dramatically, including not only “life-style” products, such as potency enhancing drugs, but also vital medicines for the treatment of e.g. high blood pressure, erectile dysfunction or high cholesterol [1–4]. Besides the threat to public health, the financial and reputational damage to pharmaceutical companies is substantial.

The definition of a “counterfeit drug” by WHO is as follows: “A counterfeit medicine is one which is deliberately and fraudulently mislabelled with respect to identity and/or source. Counterfeiting can apply to both branded and generic products and counterfeit products may include products with the correct ingredients or with the wrong ingredients, without active ingredients, with insufficient active ingredient or with fake packaging” [5,6]. In 2006, the WHO established the “International Medical Products Anti Counterfeiting

Taskforce (IMPACT)”. Among other things, the European Commission is an active member of IMPACT and has specifically co-funded and supported WHO in the development of the recommendation “Principles and Elements for National Legislation against Counterfeit Medical Products” [6,7]. The Commission also works together with the European Medicines Agency (EMA).

Counterfeit medicines can have serious health consequences. Drug products without an active ingredient can endanger therapeutic effects and/or cause unpredictable reactions [4]. In case of a hypertension medicine, an incorrect dose level may already cause a high risk for the patient, since vascular damage may occur and result in a heart attack or stroke. As the manufacture of counterfeit medicines is often not in accordance with current Good Manufacturing Practices (GMP), there is usually no information about the manufacturing process, appropriate hygiene and no reliable traceability of the ingredients [8].

To protect genuine pharmaceutical products, various security features on the packaging rather than the product itself have been proposed by the WHO and the European Commission: holograms or colour-shifting ink, invisible printing and digital watermarks [9,10]. For the analysis of suspect counterfeit medicines, a variety

* Corresponding author. Tel.: +49 06221 54 8335; fax: +49 06221 54 5971.
E-mail address: gabriele.reich@urz.uni-heidelberg.de (G. Reich).

of analytical techniques are in place [4,11]. Usual methods include visual controls, disintegration tests, chromatographic assays such as LC–MS for purity, potency and content uniformity, or simple colour reaction tests [5,12–14]. Most of the established methods are destructive and/or may only detect chemical differences. Vibrational spectroscopy such as single-point near-infrared spectroscopy (NIRS) has been shown to be a versatile tool for the analysis of pharmaceutical drug products [15]. It is a non-destructive analytical technique with little or no sample preparation required and enables simultaneous determination of chemical composition (e.g. the content of the active pharmaceutical ingredient, API) and physical properties such as tablet hardness [16,17]. After successful implementation of a NIRS method, the resulting economic advantages over conventional wet analytical techniques are high, since analytics can be performed efficiently. A few studies have been published describing the use of NIRS for the detection of counterfeit drugs [1,2,11,13,18–20].

Near-infrared chemical imaging (NIR-CI) is an even more powerful technique, since it combines classical spectroscopy with the ability to provide spatial information on the distribution of the components of a drug product [15,21,22]. Thus, NIR-CI has been successfully applied for drug identification [23,24] and quantification [25,26], for visualising manufacturing problems and process effects on dissolution [27–30] and for estimating homogeneity [25,31–35]. Dubois et al. [12] and Wolff et al. [36] have used NIR-CI for the identification and characterisation of counterfeit drug products. Furthermore, a study published by the FDA [31] pointed to the additional information contained in NIR chemical images of tablets purchased on the internet, and the potential value of this additional knowledge in qualifying both the potency and the quality of the formulation as a whole [12]. Previous studies [12,36] frequently used image analysis tools such as the evaluation of mean values and % standard deviation of predicted classification scores of the components within a sample to evaluate homogeneity as a key indicator for the identification of counterfeits. Unfortunately, this approach uses the unique spatial information given by NIR-CI incompletely.

In this work, we present a new four-stage concept for the reliable identification of solid counterfeits which are very similar to the genuine product. The study is based on real samples which were investigated via NIRS and NIR-CI. A novel approach of NIR-CI data processing was applied.

2. Experimental

2.1. Materials

The motivation for this study was a confiscated blister pack with light yellow, heart-shaped, biconvex, scored tablets of a hypertension drug (bisoprolol-hemifumerate). The blister was labelled with the trade name Concor®5 of Merck KGaA. There was strong suspicion of counterfeiting, since previous investigations using LC–MS revealed a different impurity profile (data not shown), but a comparable content of bisoprolol-hemifumerate. Four tablets were taken from the blister and used for NIRS and NIR-CI analysis. All impurities were below the near-infrared detection limit.

A total of 25 tablets of the genuine drug product (Concor®5, Merck KGaA) were used as reference. The sample set included samples from various batches of two different manufacturing sites and samples collected from stability testing, thus covering product performance variability: 10 tablets from two batches produced in 2005 at Merck-site-A (stability samples with high water content determined by Karl Fischer titration); 15 tablets from three batches produced in 2008 at Merck-site-A; five tablets from one batch of Merck-site-B produced in 2006. This sample selection is in accordance with the Quality by Design (QbD) principles of the ICH

Q8 guideline “Pharmaceutical Development” [37], saying that it is essential to know the product variability.

In addition, we used a total of 30 generic tablets from five different suppliers with the same content of the active ingredient (bisoprolol-hemifumerate) as the genuine product, but differences in the excipient composition. Each generic batch consisted of five tablets. Coating was carefully removed using a scalpel in order to expose the interior to spectroscopic measurements and chemical imaging.

2.1.1. Pure components for the hyperspectral library

The genuine drug product contains bisoprolol-hemifumerate as active pharmaceutical ingredient (API) and crospovidone, microcrystalline cellulose, corn starch and calcium hydrogen phosphate as major excipients. Bisoprolol-hemifumerate (1-[4-[2-(1-methylethoxy)ethoxymethyl]phenoxy]-3-(1-methylethylamino)propan-2-ol) is a competitive, beta(1)-selective (cardioselective) adrenergic antagonist. It is used to treat hypertension, arrhythmias, coronary heart disease, glaucoma, and is also used to reduce non-fatal cardiac events in patients with heart failure [38]. Pure component spectra were collected from powder samples of bisoprolol-hemifumerate (Merck & Cie KG, Aldorf, Switzerland) and pharmaceutical grade crospovidone, microcrystalline cellulose and corn starch. Due to its low NIR activity, calcium hydrogen phosphate was not included in the hyperspectral library. Subsequently, bisoprolol-hemifumerate will be abbreviated as bisoprolol.

2.2. Methods

2.2.1. Near-infrared spectroscopy

NIR spectra of the tablets were collected in reflectance mode using (a) the Multi Purpose FT-NIR Analyser in combination with OPUS 6.5 software (both Bruker Optics, Ettlingen, Germany) and equipped with a RT-PbS detector and a 30-position automatic sample tray. The acquisition parameters were 32 scans per spectrum over the wavelength range 833–2857 nm ($12000\text{--}3500\text{ cm}^{-1}$) at a resolution of 8 nm. All tablets were equally positioned to minimise score-line effects. Furthermore, NIR spectral images of the tablets were collected in reflectance mode using (b) the SyNIRgi™ Chemical Imaging System. Data acquisition will be described in detail in the next section.

To discriminate among genuine-, generic- and counterfeit tablets, spectral data were chemometrically processed and visualised using The Unscrambler® 9.7 (Camo Software AS., Oslo, Norway) and JMP® 8 (SAS Institute Inc., Cary, USA) software, respectively. The following mathematical transformations of the spectra were successively carried out: for method (a): unit vector normalisation and extended multiplicative scatter correction (EMSC) and for method (b): unit vector normalisation and a second derivative algorithm (Savitzky–Golay algorithm [39], using third-order polynomials across 11 data points). EMSC is a powerful pre-processing technique to isolate and remove complicated multiplicative and additive effects, such as those caused by light scattering in reflectance spectroscopy. It expands on the popular multiplicative scatter/signal correction technique by offering much improved flexibility in selecting backgrounds to subtract known interferences as well as scaling targets and known analyte spectra [40,41].

Further transformations were carried out (data not shown), however, the previously mentioned methods revealed the best results.

2.2.2. Near-infrared chemical imaging

Data were collected with a SyNIRgi™ Chemical Imaging System (Malvern Instruments, Malvern, UK) equipped with an InSb

focal plane array detector (320 × 256 pixels) and a 30-position automatic sample holder. Image cubes of each tablet were acquired with Pixys[®] 1.1 software (Malvern Instruments, Malvern, UK) in the spectral range 1200–2400 nm at 10 nm steps and 16 frames per wavelength. The field of view was set to 12.8 mm × 10.2 mm which encompasses 100% of the area of the tablet and provides a magnification of 40 μm per pixel. Each image cube contained 81 920 full NIR spectra and required a collection time of approximately 3 min. Before the actual sample is scanned, the software enforces the collection of appropriate dark and background data cubes, and then uses these data to produce reflectance spectra according to the formula $R = (S - D)/(B - D)$, where S is the sample cube, B is the 99% reflectance cube (Background), D is the dark cube, and R is the resulting reflectance cube. This calculation was performed for all pixels in all planes in the cube.

Imaging data were analysed and processed with ISys 5.0 Software (Malvern Instruments, Malvern, UK). The first step was to convert the data into absorbance units according to the following equation: $A = \log 1/R$, where A = absorbance and R = reflectance. A second derivative algorithm was applied (Savitzky–Golay algorithm [39], using third-order polynomials across 11 data points). Pure component imaging data was collected from powder samples of the API and three major excipients (crospovidone, microcrystalline cellulose and corn starch). Spectral data of all four components were processed in the same manner. A reference library with >5000 spectra per component was built for the API and the excipients. These training spectra were used as predictors to build a partial least squares (PLS) classification model, which was applied to the spectral data of the tablets for discriminant analysis. For quantification purposes and/or predictions on physical attributes the validity of using powder samples of pure components as training spectra for tablet analysis may be less straightforward than in the present study, which focussed on fast discrimination between genuine and counterfeit tablets. Applying such PLS model to the tablets resulted in a “classification scores image” for each of the library components without any quantitative calibration set being required. The intensity of each pixel in the resultant predicted classification scores image is determined by the degree of membership (scaled from 0 to 1) predicted for the spectrum at that special loca-

tion based on the reference spectra [29]. A score value of 0 meant that the component was not present and a score value of 1 meant that the component was present at 100%. The brighter the colour of the pixel, the stronger the degree of membership of that spectrum to the specific class predicted at that location. For the presented images, the brighter colour represents a higher concentration. The variation in predicted classification scores and the distribution of pixels reflects the variation in component concentration across the sample and is an indication for homo-/heterogeneity. All PLS predicted images shown in the next section result from histogram plots centred to the mean and normally distributed. The predicted concentration threshold was set to 3SD.

3. Results and discussion

3.1. Stage concept

In this study, a four-stage concept for the reliable identification of solid counterfeits was developed. This new concept is shown in Fig. 1 and will be discussed in more detail in the next sections.

3.1.1. Stage 1: visual characterisation

Upon visual inspection, the confiscated blister and the tablets could not be distinguished from the genuine product: the blister was labelled with “Concor[®]5 Merck” and the tablets were light yellow, heart-shaped, both sides convex and scored as the brand. Because of the similarities of the counterfeits and the genuine tablets a multivariate NIRS/NIR-CI (PCA) analysis was performed (stage 2).

3.1.2. Stage 2: NIRS/NIR-CI analysis (PCA)

NIR spectra of genuine-, generic- and fake tablets were collected with a FT-NIR spectrometer and a NIR-imaging system. To understand the results obtained with these two techniques, the main differences between the two have to be considered. The imaging system allowed the whole tablet surface (a mean of 81 920 spectra) to be analysed, whereas a spectrum obtained from the FT-NIR spectrometer was a mean of 32 scans, given by a smaller area of the tablet surface (~3 mm). The resolution of the FT-NIR spectrometer

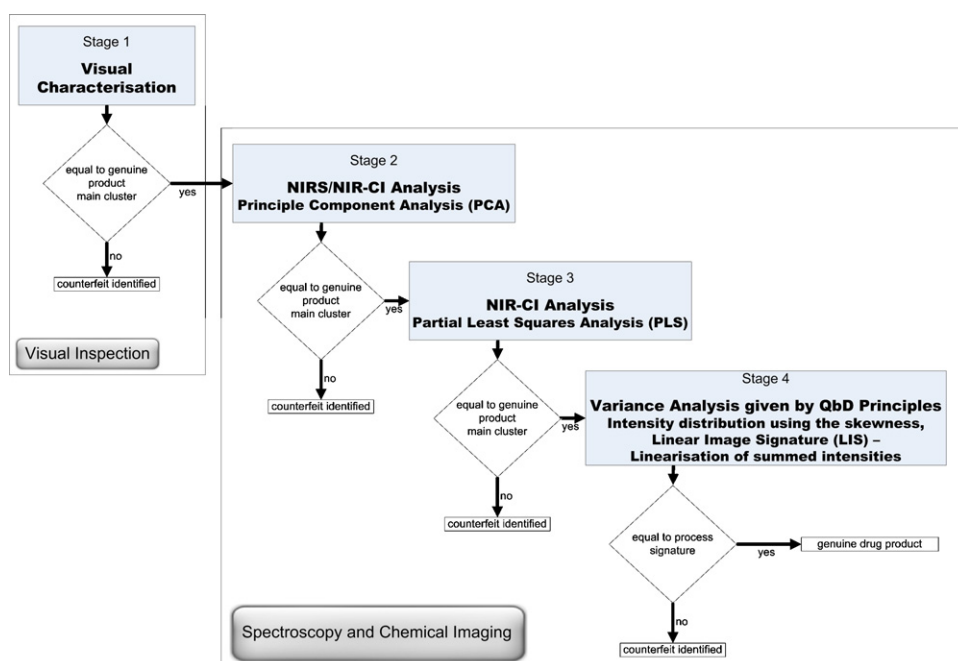


Fig. 1. General approach for the identification of counterfeit tablets.

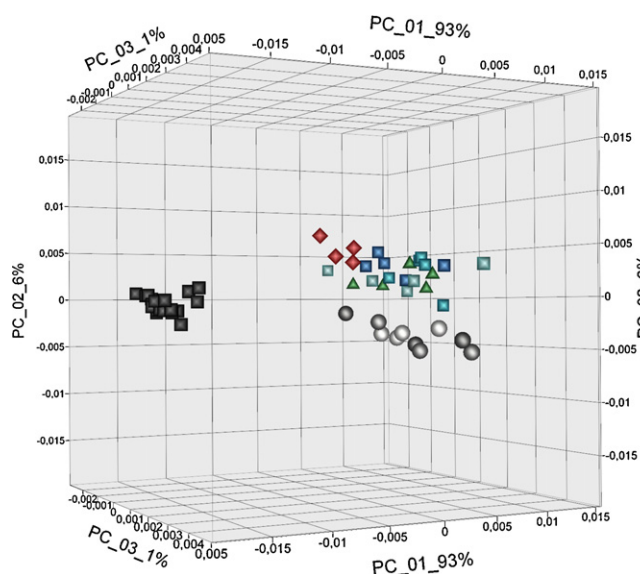


Fig. 2. Scores plot resulting from a PCA of spectra, generated by the FT-NIR spectrometer (pre-processed according to method (a)): generics produced in 2008 (black squares); wet genuine tablets produced in 2005 (circles, grey); genuine tablets produced in 2008 (squares, blue); tablets from another Merck-site produced in 2006 (triangle, green); counterfeit tablets (squares, red). (For interpretation of the references to colour in this figure legend, the reader is referred to the web version of the article.)

was higher (8 nm) and the spectral range broader (833–2857 nm) compared to the NIR-imaging system (10 nm; 1200–2400 nm).

A principal component analysis (PCA) was performed to the pre-processed spectra, collected with the FT-NIR spectrometer. Fig. 2 shows the scores plot with the first three principle components.

The scores plot clearly reveals that the counterfeit cluster is very close to the main genuine cluster and cannot be distinguished from the different genuine products. However, the cluster of the generic tablets is well separated from the cluster of the genuine product and the suspect counterfeit. This indicates compositional differences between the genuine tablets and the generics. Moreover, upon closer inspection of the genuine cluster it is evident that PC2 is able to distinguish the wet genuine tablets produced in 2005 from the remaining genuine tablets.

The results of the PCA of the pre-processed spectra collected by the NIR-imaging system are illustrated in Fig. 3.

As appears, the cluster of the counterfeit tablets is slightly separated, but still close to the main genuine cluster. Moreover, not only differences in water content (as observed in Fig. 2), but also site-to-site variability of the genuine product are distinguished. Obviously, the spectral information gained from the whole tablet surface was slightly different to the one gained from a 3 mm spot. Thus, it could be speculated that the formulation of the counterfeit tablets were different to the generic tablets.

A PCA model, which included only genuine tablets and excluded generics, was performed and applied to the counterfeit tablets. Three of four counterfeits were found inside the range of the 95% confidence interval (data not shown). Moreover, a PCA only using the spectral range related to water (~1930 nm) revealed a clear distinction between wet genuine tablets produced in 2005 and the remaining genuine tablets. The counterfeits were located near the wet genuine tablets produced in 2005 (data not shown). These results clearly show the importance of using tablets not only from different sites, but also originating from stability testing, to verify genuine product variability.

According to the developed stage concept, the counterfeit tablets were not yet identified by the use of NIRS analysis. There-

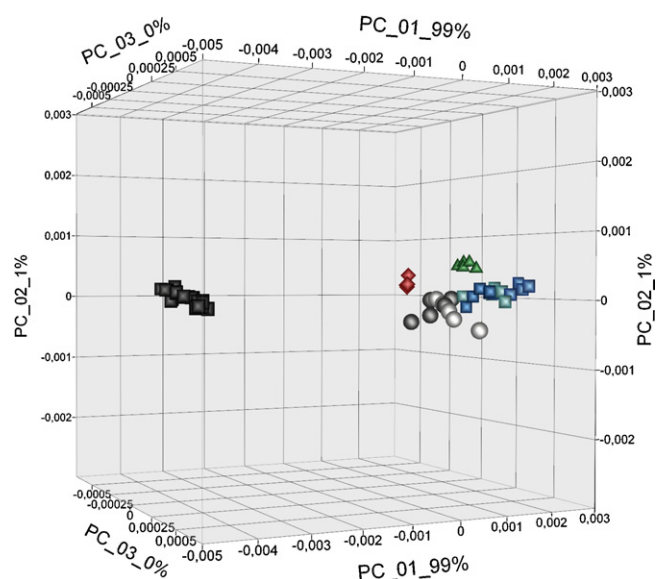


Fig. 3. Scores plot resulting from a PCA of spectra, generated by the Imaging System (pre-processed according to method (b)): generics produced in 2008 (black squares); wet genuine tablets produced in 2005 (circles, grey); genuine tablets produced in 2008 (squares, blue); tablets from another Merck-site produced in 2006 (triangle, green); counterfeit tablets (squares, red). (For interpretation of the references to colour in this figure legend, the reader is referred to the web version of the article.)

fore a more detailed NIR-CI (PLS) investigation was performed in stage 3.

3.1.3. Stage 3: NIR-CI analysis (PLS)

The first step was the development of the reference library and the PLS calibration model with the powder samples of the pure API and three major NIR-active excipients (croscopovidone, microcrystalline cellulose and corn starch). As it was the purpose of the study to establish a fast and economic method for discriminant analysis, i.e. identification of counterfeits, a PLS classification model rather than a quantitative PLS model was developed. Fig. 4a shows the PLS predicted images of the ingredients in a genuine tablet. The four components can be clearly analysed. Similarly, Fig. 4b shows related PLS predicted images for the same ingredients in a counterfeit tablet. In our case, five factors included in the model were enough for the reliable prediction of ingredients. The Predicted

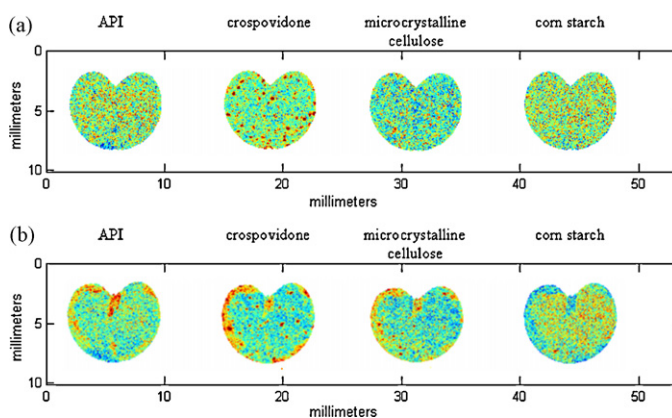


Fig. 4. Exemplary PLS predicted images: (a) genuine tablet; (b) counterfeit tablet – red pixels indicate higher concentration and blue pixels indicate lower concentration; images result from histogram plots centred to the mean and normally distributed; predicted concentration threshold: 3SD. (For interpretation of the references to colour in this figure legend, the reader is referred to the web version of the article.)

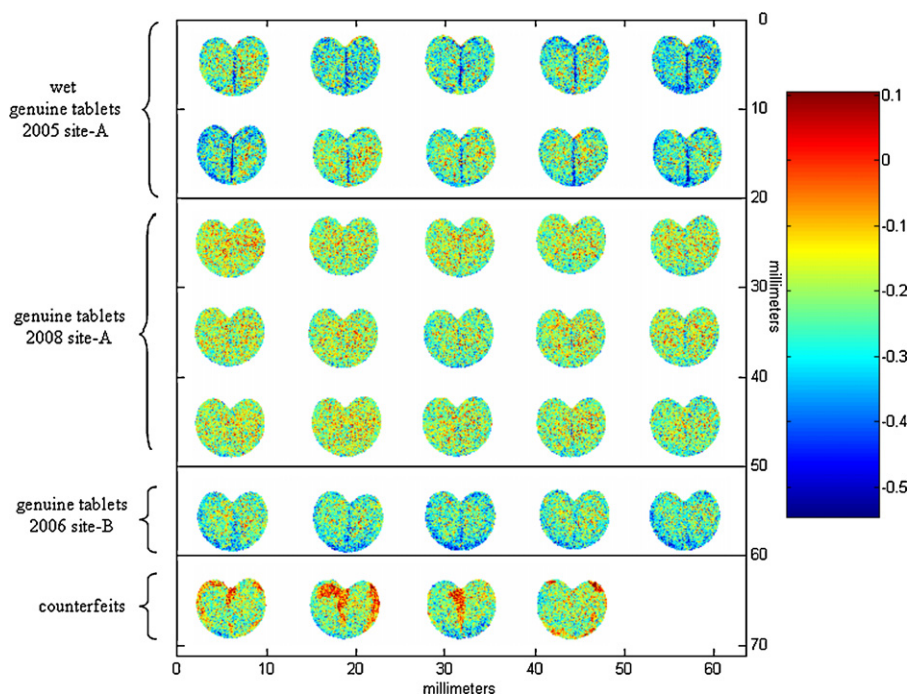


Fig. 5. PLS predicted API images for wet genuine tablets produced in 2005; genuine tablets produced in 2008; tablets from another Merck-site produced in 2006; counterfeit tablets – red pixels indicate higher concentration and blue pixels indicate lower concentration; images result from histogram plots centred to the mean and normally distributed; predicted concentration threshold: 3SD. (For interpretation of the references to colour in this figure legend, the reader is referred to the web version of the article.)

Residual Sum of Squares (PRESS) was lower than 0.02 at that stage. PRESS displays how the residual prediction errors depend on the number of factors in the model. We truncated the factors beyond five because the slope of the PRESS significantly flattens. This flattening of the slope indicates that the subsequent factors contribute little to the prediction.

The NIR-CI results demonstrate the ability of the imaging system to detect the API and the major excipients and display its spatial distribution within the drug product. As the genuine product, the counterfeit tablets consist of bisoprolol, crospovidone, microcrystalline cellulose and corn starch, in a similar relative abundance.

The next step was to apply the PLS model to all tablets. In order to minimise the complexity we continued with the API and the major excipient crospovidone. Calculations were also performed for the other two major excipients (data not shown).

Fig. 5 shows the PLS predicted API images for the genuine drug products and counterfeit tablets. The score values over the images show that the maximum value at any pixel is only ~ 0.1 which would equate to an abundance of $\sim 10\%$, i.e. 90% of the pixel contribution is from the other components.

The API is well distributed throughout the original product, but not in the counterfeits. Regions of high concentration, indicating a lack of mixing, were more prevalent in the counterfeit drug product than in the genuine tablets, indicating poor API homogeneity in the counterfeit. Generally, all samples from a given batch were similar.

Fig. 6 shows the PLS predicted crospovidone images in genuine drug products and counterfeits. Crospovidone as a disintegrant plays a major role in a tablet formulation. A disintegrant is an excipient which is added to a tablet or a powder blend of a capsule to assist disintegration of the compacted mass when it gets in contact with an aqueous medium. Crospovidone is completely insoluble in water but it rapidly swells in water [42,43]. In our case, the swollen crospovidone in wet tablets caused changes in the matrix of the tablet, which result in higher predicted classification score values (Fig. 6).

The visual inspection of the images already indicates differences in the homogeneity of the samples according to the API and the crospovidone. The measurement of the homogeneity could be an effective way to identify counterfeits. Lyon et al. [32] describe homogeneity measurements by calculating the % standard deviation of the distribution of the predicted classification scores for a given component within a specimen. Homogeneous tablets will have small standard deviations, while heterogeneous tablets will have larger standard deviations. Image statistics was carried out, but the % standard deviation of the predicted classification scores for the API was less sensitive. There was no major difference between the average % standard deviation for the genuine tablets (5.78 ± 0.6) and the counterfeit tablets (8.58 ± 0.9).

Since stage 3 (i.e. NIR-CI (PLS) analysis) revealed that the composition of the counterfeits is very similar to the genuine drug product, a new statistic approach was used to analyse sample variability, i.e. homogeneity. The approach will be discussed in more detail in the next section.

3.1.4. Stage 4: variance analysis given by Quality by Design (QbD) principles

The sample set of the genuine product including intra-batch, batch-to-batch and site-to-site variabilities resulted in an image signature which allowed the product variability to be identified according to the Quality by Design (QbD) principles of the ICH Q8 [37] guideline. In a study, initiated by the Office of Compliance in FDA's Center for Drug Evaluation and Research, Westenberger et al. [31] investigated the use of non-traditional analytical methods like NIRS and NIR-CI to evaluate the quality of a variety of pharmaceutical products. One result of the study was emphasised: "To identify an entire sample lot as less homogeneous than the innovator, it would be necessary to examine multiple lots of innovator product to determine a range of acceptable variability" [31].

We performed sample statistics by the use of the software ISys, which is an important tool in the visualisation of imaging data.

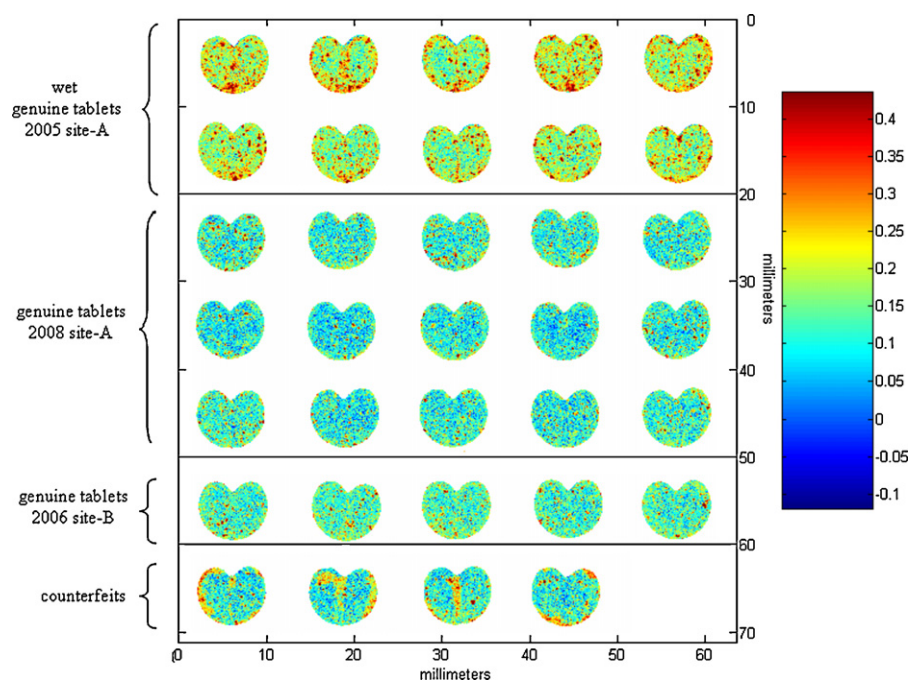


Fig. 6. PLS predicted crosopvidone images for wet genuine tablets produced in 2005; genuine tablets produced in 2008; tablets from another Merck-site produced in 2006; counterfeit tablets – red pixels indicate higher concentration and blue pixels indicate lower concentration; images result from histogram plots centred to the mean and normally distributed; predicted concentration threshold: 3SD. (For interpretation of the references to colour in this figure legend, the reader is referred to the web version of the article.)

Through histogram plots and statistics patterns the predicted classification scores and pixel distribution throughout the image can be computed. One parameter given by the histogram plot is skewness, which can be used as supportive information to interpret the distribution of a component. Skewness is a measure of lack of symmetry; it indicates whether the distribution is symmetrical to the centre of mass of the histogram plot. A normal distribution with close-to-zero skewness is generally indicative of good homogeneity. A negative skewness indicates that the distribution is tailing to the left and a positive skew indicates tailing to the right. They are both often related to inhomogeneity in the sample and therefore could be used for diagnosing counterfeiting. Another parameter given by the histogram plot is kurtosis. It is a measure of the flatness or

“peakedness” of the distribution and can also be used as indicator of homogeneity. In our case, however, we observed that the kurtosis was less sensitive than skewness (data not shown). This may be different in case of other samples.

The skewness value of the API was plotted against the skewness value of crosopvidone to show the heterogeneity within the tablets (Fig. 7). It is evident that the counterfeits have higher skewness values of the API. This result confirms the visual observation of the chemical images in stage 3. The counterfeits are less homogeneous with respect to the API distribution than the genuine tablets.

Based on these results, a new approach to determine product variabilities was attempted, namely to sum up the predicted classification scores of the PLS predicted API image. The procedure

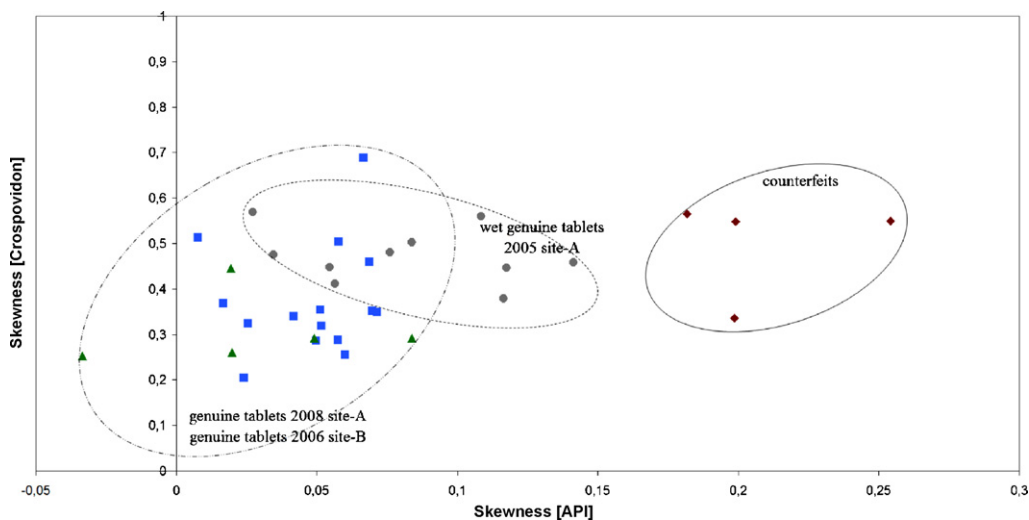


Fig. 7. Skewness values of the API vs. skewness values of crosopvidone: wet genuine tablets produced in 2005 (circles, grey); genuine tablets produced in 2008 (squares, blue); tablets from another Merck-site produced in 2006 (triangle, green); counterfeit tablets (squares, red). (For interpretation of the references to colour in this figure legend, the reader is referred to the web version of the article.)

will be exemplarily described by means of one tablet as shown in Fig. 8a.

The first step was to export the PLS predicted API image as ASCII-file to a spreadsheet-application software. We used a definite range of positive classification scores (0–0.1) for better comparability. This resulted in a data set with ~168 rows and 196 columns of classification scores per tablet (similar “heart-shape” of the used tablets). Next, the sums over the scores (concentrations) were simply calculated column by column (X-direction) and line by line (Y-direction). For ease of understanding the worksheet was turned by 90 degrees as displayed in Fig. 8a (right side). The Z-direction represents the predicted concentrations. The concatenation of the received X- and Y-dimension data in one row resulted in an unfolding of information, i.e. a Linear Image Signature (LIS). Fig. 8b illustrates the X- and Y-values of four tablets in a line plot. Fig. 8c represents the corresponding first derivative (Savitzky–Golay algorithm [39], using second-order polynomials across 25 data points). To classify different signatures, a PCA was applied to the LIS profiles (Fig. 9).

The small distance between the genuine tablet batches reflects their similarity. The counterfeits, however, are now far apart. This is in contrast to the results obtained from NIRS measurements based on both acquisition and pre-processing methods tested (i.e. (a) and (b)) and a clear indication of counterfeiting. With the new approach it was possible to distinguish among the innovator product and the counterfeit tablets because spatial information obtained by NIR-Cl

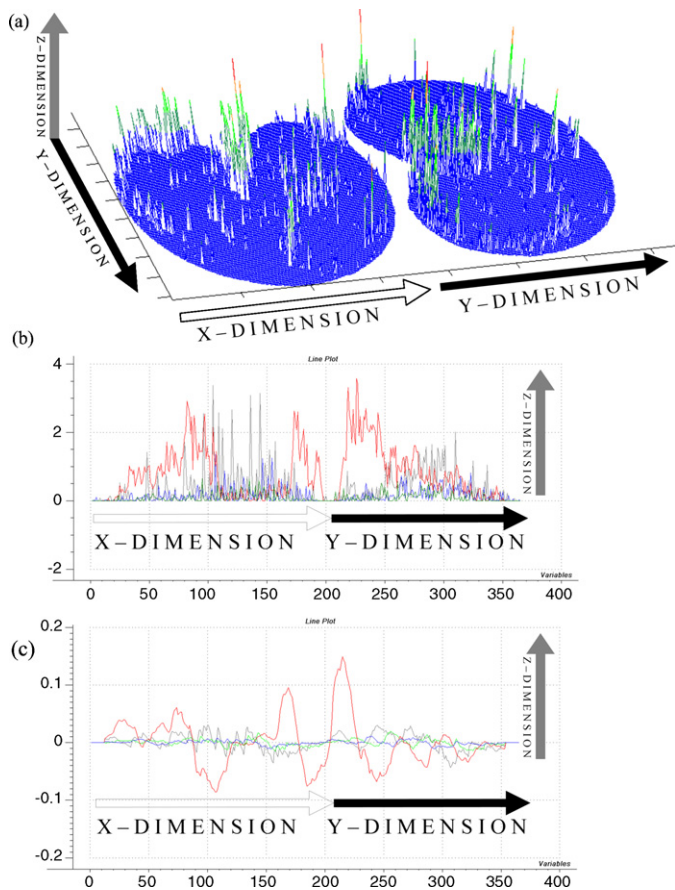


Fig. 8. (a) Exemplary description of summation of the predicted classification scores of one PLS predicted API image column by column; (b) line plot of the sums of X- and Y-values of the predicted classification scores of the PLS predicted API images – counterfeit (red), wet genuine tablet produced in 2005 (grey), genuine tablet produced in 2008 (blue), genuine tablet of another Merck-site (green); (c) first derivative data of (b). (For interpretation of the references to colour in this figure legend, the reader is referred to the web version of the article).

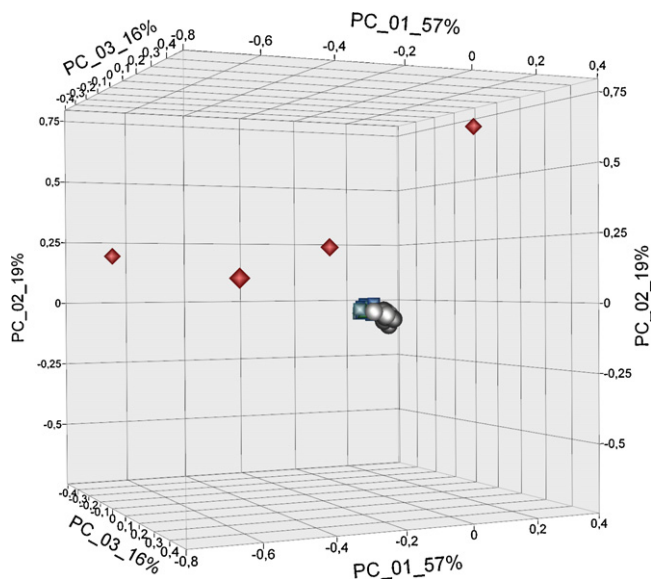


Fig. 9. Scores plot resulting from a PCA of summed and unfolded classification scores of the PLS predicted API images: wet genuine tablets produced in 2005 (circles, grey); genuine tablets produced in 2008 (squares, grey); tablets from another Merck-site produced in 2006 (triangle, green); counterfeit tablets (squares, red). (For interpretation of the references to colour in this figure legend, the reader is referred to the web version of the article.)

was combined with information on product variability. The proposed method may be complemented with adequate statistical criteria (e.g. multivariate Hotelling T^2 statistics) for discrimination.

4. Conclusions

A new stage concept for the reliable identification of solid counterfeits was developed. Based on real samples it was demonstrated that this stage concept works for counterfeits which are very similar to the genuine product. Single-point NIRS has been shown to be a highly efficient technique for differentiating between the innovator product and generic tablets with compositional differences (e.g. different major excipients). For counterfeit identification, NIR-Cl turned out to be superior to single-point NIRS because it combines the capability of spectroscopy with the potential of visualisation, thus allowing local characterisation of the chemical composition, domain structure, and chemical architecture. In addition, it delineates the spatial uniformity of the API as well as major excipients across the final dosage form, and the whole tablet surface is ascertainable. For the present study we used homogeneity as a key indicator for the identification of counterfeits. It was shown that the skewness of pixel distribution given by the image statistics is a meaningful quality parameter to describe homogeneity. However, the disadvantage of this approach is the partial loss of spatial information.

Therefore, we developed a new method that uses the spatial information for the evaluation of homogeneity by means of summation and unfolding of multidimensional predicted concentrations (i.e. values for a given specimen in a predicted image). This approach results in a Linear Image Signature (LIS) which contains spatial information despite linearisation. Multivariate LIS data analysis revealed higher variability in pixel distribution and predicted concentrations for the counterfeit tablets compared to the genuine product, and thus allowed to successfully identify the counterfeit tablets.

Detection of product variability by this novel procedure is an interesting approach not only for counterfeit identification, but also for process validation, i.e. to determine the process signature of

pharmaceutical dosage forms. The use of LIS for monitoring powder blend uniformity is part of ongoing QbD experiments.

Acknowledgments

The authors want to thank Dr. Robert Nass and Dr. Jens Schewitz from Merck Serono for their overall support of the project. Furthermore, we want to thank Sandra Kuhn, Melanie Kowollik, Thorsten Herdling and in particular Emeline Roux from Merck Serono PAT-Laboratory Darmstadt for their friendly and kind help and fruitful discussions.

References

- [1] M.J. Vredendregt, D. Mooiroek, R. Hoogerbrugge, Your viagrass—genuine, imitation, or counterfeit? in: D.A. Burns, E.W. Ciurczak (Eds.), *Handbook of Near-Infrared Analysis*, CRC Press, Boca Raton, 2007, pp. 631–646.
- [2] M.J. Vredendregt, L. Blok-Tip, R. Hoogerbrugge, D.M. Barends, D.D. Kaste, Screening suspected counterfeit viagra(R) and imitations of viagra(R) with near-infrared spectroscopy *J. Pharm. Biomed. Anal.* 40 (2006) 840–849.
- [3] S. Singh, B. Prasad, A.A. Savaliya, R.P. Shah, V.M. Gohil, A. Kaur, Strategies for characterizing sildenafil, vardenafil, tadalafil and their analogues in herbal dietary supplements, and detecting counterfeit products containing these drugs, *Trends Anal. Chem.* 28 (2009) 13–28.
- [4] A.K. Deisingh, Pharmaceutical counterfeiting, *Analyst* 130 (2005) 271–279.
- [5] World Health Organization, *Counterfeit Drugs—Guidelines for the Development of Measures to Combat Counterfeit Drugs*, WHO, Geneva, 1999, pp. 1–62.
- [6] International Medical Products Anti-Counterfeiting Taskforce, *Principles and Elements for National Legislation against Counterfeit Medical Products*, IMPACT General Meeting Lisbon, 2007, pp. 1–13.
- [7] http://ec.europa.eu/enterprise/pharmaceuticals/counterf.par.trade/counterfeit_en.htm (2009) 1–1.
- [8] U.S. Department of Health and Human Services: Food and Drug Administration, *Guidance for Industry: Quality Systems Approach to Pharmaceutical CGMP Regulations*, 2006, pp. 1–32.
- [9] World Health Organization, *Forty-second Report of the WHO Expert Committee on Specifications for Pharmaceutical Preparations*, WHO Technical Report Series, No. 948 (2008) 1–150.
- [10] European Commission, *Preparation of a Legislative Proposal to Combat Counterfeit Medicines for Human Use*, Summary of Responses to the Public Consultation Document, Brüssel, 2008, pp. 1–11.
- [11] B.A. Olsen, M.W. Borer, F.M. Perry, R.A. Forbes, Screening for counterfeit drugs using near-infrared spectroscopy, *Pharm. Technol.* 26 (2002) 62–71.
- [12] J. Dubois, J.-C. Wolff, J.K. Warrack, J. Schoppelrei, E.N. Lewis, NIR chemical imaging for counterfeit pharmaceutical products analysis, *Spectroscopy* (2007) 40–46.
- [13] O.Y. Rodionova, L.P. Houmøller, A.L. Pomerantsev, P. Geladi, J. Burger, V.L. Dorofeyev, A.P. Arzamastsev, NIR spectrometry for counterfeit drug detection: a feasibility study, *Anal. Chim. Acta* 549 (2005) 151–158.
- [14] World Health Organization, *Basic Tests for Drugs: Pharmaceutical Substances, Medicinal Plant Materials and Dosage Forms*, WHO, Geneva, 1998, pp. 1–94.
- [15] C.A. Anderson, J.K. Drennen, E.W. Ciurczak, Pharmaceutical applications of near-infrared spectroscopy, in: D.A. Burns, E.W. Ciurczak (Eds.), *Handbook of Near-Infrared Analysis*, CRC Press, Boca Raton, 2007, pp. 585–612.
- [16] M. Blanco, M. Alcalá, J.M. González, E. Torras, A process analytical technology approach based on near infrared spectroscopy: Tablet hardness, content uniformity, and dissolution test measurements of intact tablets, *Wiley InterScience* 95 (2006) 2137–2144.
- [17] D. Filmore, Keeping an (infrared) eye out, in: *Modern Drug Discovery* September, 2003, pp. 35–40.
- [18] P. de Peinder, M.J. Vredendregt, T. Visser, D. de Kaste, Detection of Lipitor® counterfeits: a comparison of NIR and Raman spectroscopy in combination with chemometrics, *J. Pharm. Biomed. Anal.* 47 (2008) 688–694.
- [19] S.H.F. Scafi, C. Pasquini, Identification of counterfeit drugs using near-infrared spectroscopy, *Analyst* 126 (2001) 2218–2224.
- [20] W.L. Yoon, Near-infrared spectroscopy: a novel tool to detect pharmaceutical counterfeits, *Am. Pharm. Rev.* (2008) 115–118.
- [21] G. Reich, Near-infrared spectroscopy and imaging: basic principles and pharmaceutical applications, *Adv. Drug Deliv. Rev.* 57 (2005) 1109–1143.
- [22] J. Burger, P. Geladi, Hyperspectral NIR imaging for calibration and prediction: a comparison between image and spectrometer data for studying organic and biological samples, *Analyst* 131 (2006) 1152–1160.
- [23] F. Clarke, Extracting process-related information from pharmaceutical dosage forms using near infrared microscopy, *Vib. Spectrosc.* 34 (2004) 25–35.
- [24] E.N. Lewis, J. Schoppelrei, E. Lee, Near-infrared chemical imaging and the PAT initiative, *Spectroscopy* (2004) 26–34.
- [25] C. Gendrin, Y. Roggo, C. Collet, Pharmaceutical applications of vibrational chemical imaging and chemometrics: a review, *J. Pharm. Biomed. Anal.* 48 (2008) 533–553.
- [26] E. Lee, W.X. Huang, P. Chen, E.N. Lewis, R.V. Vivilecchia, High-throughput analysis of pharmaceutical tablet content uniformity by near-infrared chemical imaging, *Spectroscopy* 21 (2006) 24–31.
- [27] Y. Roggo, A. Edmond, P. Chalus, M. Ulmschneider, Infrared hyperspectral imaging for qualitative analysis of pharmaceutical solid forms, *Anal. Chim. Acta* 535 (2005) 79–87.
- [28] J. Dubois, E.N. Lewis, *Advanced Troubleshooting of Dissolution Failure*, 2009, pp. 38–45. Available from: www.pharmaceuticalonline.com.
- [29] L. Makein, L.H. Kidder, E.N. Lewis, M. Valleri, Non-destructive evaluation of manufacturing process changes using near infrared chemical imaging, *NIR News* 19 (2008) 11–15.
- [30] Y. Roggo, N. Jent, A. Edmond, P. Chalus, M. Ulmschneider, Characterizing process effects on pharmaceutical solid forms using near-infrared spectroscopy and infrared imaging, *Eur. J. Pharm. Biopharm.* 61 (2005) 100–110.
- [31] B.J. Westenberger, C.D. Ellison, A.S. Fussner, S. Jenney, R.E. Kolinski, T.G. Lipe, R.C. Lyon, T.W. Moore, L.K. Revelle, A.P. Smith, J.A. Spencer, K.D. Story, D.Y. Toler, A.M. Wokovich, L.F. Buhse, Quality assessment of internet pharmaceutical products using traditional and non-traditional analytical techniques, *Int. J. Pharm.* 306 (2005) 56–70.
- [32] R.C. Lyon, D.S. Lester, E.N. Lewis, E. Lee, L.X. Yu, E.H. Jefferson, A.S. Hussain, Near-infrared spectral imaging for quality assurance of pharmaceutical products: analysis of tablets to assess powder blend homogeneity, *AAPS Pharm. Sci. Technol.* 3 (2002) 1–15.
- [33] C. Gendrin, Y. Roggo, C. Spiegel, C. Collet, Monitoring galenic process development by near infrared chemical imaging: one case study, *Eur. J. Pharm. Biopharm.* 68 (2008) 828–838.
- [34] E.N. Lewis, J.E. Carroll, F. Clarke, A near infrared view of pharmaceutical formulation analysis, *NIR News* 12 (2001) 16–18.
- [35] A.S. El-Hagrasy, H.R. Morris, F. D'Amico, R.A. Lodder, J.K. Drennen III, Near-infrared spectroscopy and imaging for the monitoring of powder blend homogeneity, *J. Pharm. Sci.* 90 (2001) 1298–1307.
- [36] J.-C. Wolff, J.K. Warrack, L. Kidder, E.N. Lewis, NIR-based chemical imaging as an anticounterfeiting tool, *Pharm. Manuf.* 7 (2008) 27–31.
- [37] International Conference of Harmonisation, *ICH Q8: Pharmaceutical Development: Step 4*, 2005, pp. 1–11.
- [38] E. Mutschler, G. Geisslinger, H.K. Kroemer, M. Schäfer-Korting, β -Adrenoceptor-antagonisten, in: E. Mutschler, G. Geisslinger, H.K. Kroemer, M. Schäfer-Korting (Eds.), *Mutschler Arzneimittelwirkungen*, Wissenschaftliche Verlagsgesellschaft mbH, Stuttgart, 2001, pp. 342–348.
- [39] A. Savitzky, H.J.E. Golay, Smoothing and differentiation of data by simplified least squares procedures, *Anal. Chem.* 36 (1964) 1627–1639.
- [40] Eigenvector Research Inc., Available from: <http://software.eigenvector.com/toolbox/emsc/toolbox/index.html> (2009) 1–1.
- [41] H. Martens, J.P. Nielsen, S.B. Engelsen, Light scattering and light absorbance separated by extended multiplicative signal correction. Application to near-infrared transmission analysis of powder mixtures, *Anal. Chem.* 75 (2003) 394–404.
- [42] W.A. Ritschel, A. Bauer-Brandl, *Tablettenbestandteile*, in: W.A. Ritschel, A. Bauer-Brandl (Eds.), *Die Tablette*, Editio Cantor Verlag, Aulendorf, 2002, pp. 60–207.
- [43] F. Carli, F. Garbassi, Characterization of drug loading in crosopidone by X-ray photoelectron spectroscopy, *J. Pharm. Sci.* 74 (1985) 963–967.